*e-mail: wxj32820126.com

Radial Dynamics of Ultrasound-Driven Bubbles with Sensitivity Analysis on Liquid Physical Parameters

X. Wang a,b,* , Z. Ning b , M. Lv b , X. Wang c and C. Hu c

Received: 11.04.2025 & Accepted: 04.09.2025

Doi: 10.12693/APhysPolA.148.99

Ultrasonic bubbles exhibit radial dynamic behavior by absorbing ultrasonic energy, and this behavior depends on the specific excitation conditions and physical parameters of the liquid. In this study, the Keller–Miksis equation is applied to study the radial oscillations of bubbles, focusing on the absorbed ultrasonic energy. Furthermore, the sensitivity of bubble dynamics to physical parameters in liquids with varying viscosities is also investigated. The results demonstrate that the maximum oscillation radius, the rebound oscillation radius, the bubble collapse strength and the absorbed ultrasonic energy increase with ultrasonic pressure, while they decrease with ultrasonic frequency. Notably, with the exception of absorbed ultrasonic energy, the other three indicators exhibit an increasing–decreasing trend as the initial bubble radius increases. Additionally, liquids can be classified into low-viscosity and high-viscosity categories. The effect of liquid physical parameters on bubble collapse strength under different ultrasonic excitation conditions is complex and multifaceted. Overall, liquid viscosity is the most important factor influencing bubble collapse strength, whereas liquid density and surface tension also exert some influence under specific conditions. In contrast, ultrasonic speed has minimal impact on collapse strength.

topics: ultrasonic cavitation bubble, bubble dynamics, ultrasonic energy, sensitivity analysis

1. Introduction

Ultrasonic excitation technology serves as an efficient method of energy conversion, capable of inducing the formation, growth, and collapse of bubbles through the transmission of ultrasonic waves within a liquid medium [1, 2]. This process induces a variety of physical and chemical effects that have been widely utilized in industrial and medical applications [3–7]. Research demonstrates that the radial dynamic behavior of bubbles directly influences the effectiveness of these applications [8–10]. As a result, a comprehensive investigation of acoustic bubble dynamics is of profound theoretical and practical significance. Recent advances have been made in bubble dynamics under various parameters [11–21]. Bubbles respond to the ultrasonic radiation force and exhibit both linear and nonlinear dynamics, which include main, harmonic, subharmonic, and ultraharmonic resonances. Factors influencing the bubble dynamic behavior include acoustic frequency and pressure, bubble size, and liquid properties [11–13]. To investigate the effects of these parameters over an extended range, methods based on chaos theory are used [14, 15]. Additionally, the non-equilibrium evaporation and condensation of water vapor, as well as the inner-bubble chemical reactions, also play an important role in bubble dynamics [16, 17]. Peng et al. [18] established a relationship between bubble collapse intensity and liquid temperature. Wang et al. [19] applied random forests and neural networks to examine the influence of liquid properties on bubble dynamics. However, their study did not separately analyze cases involving different ranges of liquid viscosity coefficients. Doinikov [20] developed equations based on the Lagrangian equations to describe bubble pulsation and translation. Based on Doinikov's model, Ma et al. [21] demonstrated that bubble translation depends on the distance from the pressure antinode and the primary Bjerknes force, and cavitation becomes more drastic in low-frequency, high-pressure acoustic environments.

^a Beijing Polytechnic University, School of Automobile Engineering, 100176, Beijing, China
^b Beijing, Baotong University, School of Mechanical and Electronic Control Engineering, 100014

^bBeijing Jiaotong University, School of Mechanical and Electronic Control Engineering, 100044, Beijing, China

^cChinese Academy of Sciences, State Key Laboratory of Acoustics and Marine Information, Institute of Acoustics, 100190, Beijing, China

Additionally, dual-frequency driven bubble dynamics, interactions between multiple bubbles and their dynamics, non-spherical bubble dynamics, and bubble-wall interactions are currently popular research topics [22–31]. Dual-frequency ultrasound exhibits unique interaction characteristics with bubbles, such as combination resonance of bubbles [22, 23], which can enhance the likelihood of bubble collapse [24]. Considering radiation delay, Wang et al. [25] found that when the interbubble distance is large, the total scattered field of a bubble cluster is approximately equal to the interference of multiple secondary acoustic sources. Sadighi-Bonabi [27] showed that an increase in liquid viscosity reduces the inter-bubble interactions. Wang et al. [28] revealed the transition mechanisms of bubble translational motions and identified a chaotic bubble pair. Additionally, the non-spherical deformation of bubbles significantly affects their interaction, which is associated with the bubbles shape mode, equilibrium radii, and driving condition [29, 30]. Guo et al. [31] demonstrated that walls inhibit the bubble collapse. Compared to a single bubble, the dual bubbles have higher velocities and require a narrower range of initial radii to produce microjets.

In summary, extensive research has been devoted to the study of bubble dynamics. However, to date, there has been limited research on bubble radial dynamics from the perspective of energy transfer between cavitation bubbles and ultrasonic waves. Furthermore, the synergistic effects of multiple liquid parameters remain insufficiently explored, particularly in liquids with varying viscosity. In this study, the influencing factors and laws of radial dynamics of bubbles are analyzed, with a focus on the ultrasonic energy they absorb. Additionally, the sensitivity relationship between bubble radial dynamics and physical parameters in low-viscosity and highviscosity liquids under various ultrasonic pressure and frequency conditions is discussed. The aim of this study is to further deepen our understanding of ultrasound-driven bubble oscillation, thereby providing a critical theoretical basis for the development of innovative applications of this technology across diverse fields.

2. Model and solutions

Assuming a spherical bubble geometry within an incompressible, inviscid liquid, bubbles oscillations were originally described by the classical Rayleigh equation [32]. Subsequent modifications by Plesset, Noltingk and Neppiras, and Poritsky extended this framework to account for viscous forces and surface tension, resulting in the Rayleigh–Plesset equation [33, 34]. During violent bubble oscillations, particularly at the collapse instant, the interface velocity may reach hundreds of meters per second,

reaching magnitudes comparable to the acoustic velocity of the liquid (1500 m/s in water, corresponding to $Ma \approx 0.1$ –1). At such velocities, density variations within the liquid become non-negligible, thus invalidating the conventional incompressible flow assumption. Consequently, by accounting for the compressibility of the liquid, Keller and Miksis refined the bubble dynamics equation based on the Rayleigh–Plesset equation, establishing the renowned Keller–Miksis model [35]

$$\left(1 - \frac{\dot{R}}{c}\right) R \ddot{R} + \frac{3}{2} \dot{R}^2 \left(1 - \frac{\dot{R}}{3c}\right) = \frac{P_t}{\rho} + \frac{1}{\rho c} \frac{\mathrm{d}}{\mathrm{d}t} (R P_t) =$$

$$\left(1 + \frac{\dot{R}}{c}\right) \frac{P_t}{\rho} + \frac{R}{\rho c} \frac{\mathrm{d}P_t}{\mathrm{d}t}.$$
(1)

In this model, R_0 [μ m] signifies the initial radius of the bubble, while R denotes its instantaneous radius. The bubble-wall velocity is represented by \dot{R} [μ m/s], and the rate of change of this velocity is expressed as \ddot{R} [μ m/s²]. The parameter c [m/s] refers to the speed of ultrasonic waves in the liquid, and P_v [kPa] indicates the saturated vapor pressure inside the bubble. The polytropic exponent is denoted by κ , and ρ [kg/m³], σ [N/m], and μ [Pa s] correspond to the density, surface tension, and viscosity of the liquid, respectively. In (1), P_t represents the total pressure exerted on the bubble wall. The model formulation combines both the vapor pressure terms and the adiabatic compression of the gas inside the bubble. This leads to the following equation

$$P_t = \left(P_0 - P_v + \frac{2\sigma}{R_0}\right) \left(\frac{R_0}{R}\right)^{3\kappa} + P_v + P_A(t) - \frac{2\sigma}{R}$$
$$-4\mu \frac{\dot{R}}{R} - P_0. \tag{2}$$

Here, P_0 is the static pressure [kPa], and $P_A(t)$ represents the ultrasonic pressure in the form of a sinusoidal wave and is written as

$$P_A(t) = P_a \sin(2\pi f_0 t), \qquad (3)$$

where P_a [kPa] denotes the ultrasonic pressure amplitude, and f_0 [kHz] is the ultrasonic frequency. It should be clarified that although the Keller–Miksis model takes into account the compressibility of the liquid, it may inadequately capture strong nonlinear effects during extreme compression. Complex compressibility-induced phenomena, such as rarefaction and compression waves, often violate the core hypotheses of the model. Additionally, at very high oscillation frequencies, where bubble size variations become sub-resolution within computational time steps, high-frequency instabilities may emerge, requiring specialized numerical stabilization.

The initial conditions are set such that at time t=0, the bubble radius R is equal to R_0 , and \dot{R} is zero. Deionized water at a temperature of 20°C is used as the ultrasonic excitation medium, and the following parameter values are applied: c=1500 m/s, $\rho=998$ kg/m³, $\sigma=0.0728$ N/m, $\mu=0.001$ Pa s, $P_v=2330$ Pa, $\kappa=4/3$. The effects

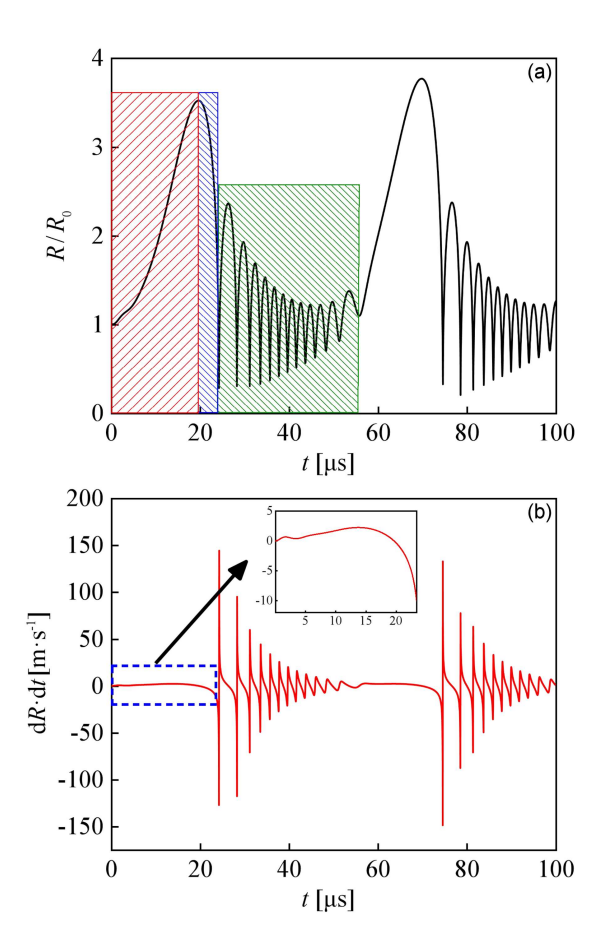


Fig. 1. The variances of (a) dimensionless oscillation radius (R/R_0) and (b) bubble-wall velocity $(\mathrm{d}R/\mathrm{d}t)$ with time (t). Here, $P_a=110$ kPa, $f_0=20$ kHz and $R_0=10~\mu\mathrm{m}$.

of ultrasonic cavitation encompass a variety of phenomena, including mechanical, thermal, chemical, and biological effects. Research findings indicate that the ultrasonic cavitation effect is closely related to the radial motion of cavitation bubbles, and especially to their collapse strength [9, 10]. The bubble collapse strength can be characterized by parameters such as the bubble expansion ratio, relative expansion ratio and compression ratio [36, 37]. In this study, the bubble expansion ratio is chosen as a parameter to characterize the collapse strength of bubbles and the effects of ultrasonic cavitation. The bubble collapse strength is defined as

$$k = \frac{R_{\text{max}}}{R},\tag{4}$$

where k represents the bubble collapse strength, and $R_{\rm max}$ denotes the maximum oscillation radius of the bubble. Under ultrasonic excitation, a cavitation bubble in a liquid serves as an energy transformer. As the bubble expands, it absorbs ultrasonic energy and grows in size. During its subsequent collapse, the stored energy is rapidly released, generating significant cavitation effects. The ultrasonic energy captured by the bubble during its expansion

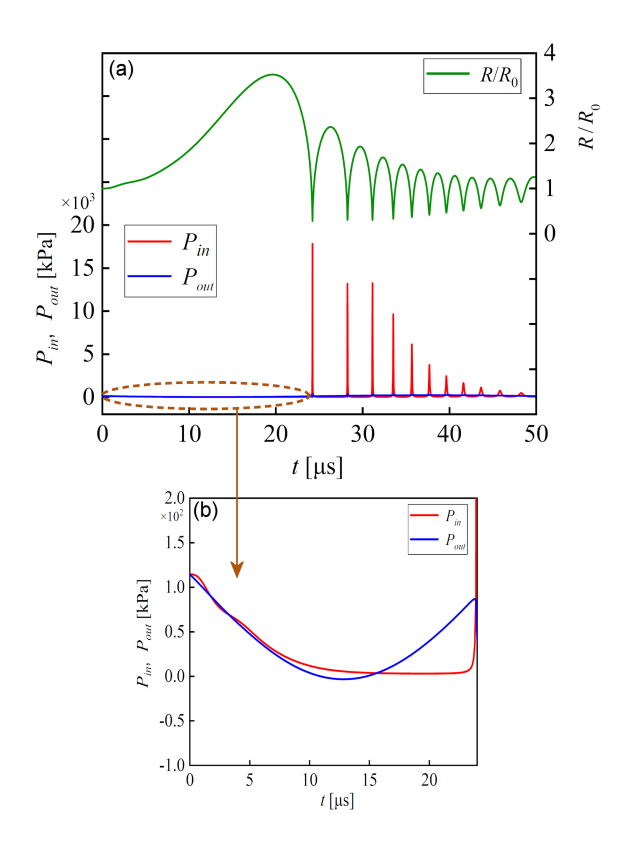


Fig. 2. (a, b) Changes in intra-bubble pressure (P_{in}) and extra-bubble pressures (P_{out}) with time (t) within one ultrasonic period. Here, $P_a=110$ kPa, $f_0=20$ kHz and $R_0=10~\mu \mathrm{m}$.

can be determined by the work required to overcome the liquid's hydrostatic pressure, viscous drag, and surface tension, i.e.,

$$E_u = \int_{R_0}^{R_{\text{max}}} dR \ 4\pi R^2 \left(P_0 + \frac{2\sigma}{R} + \frac{4\mu}{R} \frac{dR}{dt} \right), \qquad (5)$$

where E_u [J] is the ultrasonic energy absorbed by the bubble during its expansion stage.

3. Results and discussion

3.1. Radial dynamics of ultrasound-driven bubbles

Figure 1 illustrates the time-dependent variations of the dimensionless oscillation radius and wall velocity of a bubble with an initial radius of 10 μ m. The ultrasonic pressure amplitude P_a is set to 110 kPa, and the frequency f_0 is 20 kHz. The red, blue, and green shaded areas represent the expansion, collapse, and rebound attenuation phases, respectively.

Figure 1a illustrates that the bubble rapidly collapses after expanding from its initial radius to the maximum radius, and subsequently begins to oscillate around the initial radius during the rebound.

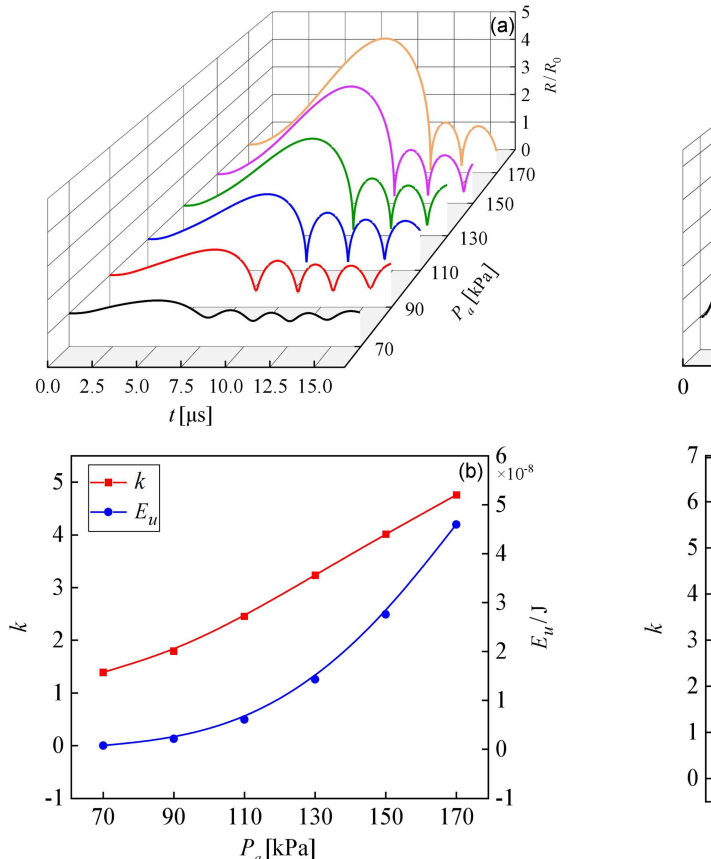


Fig. 3. (a) The time-dependent changes in the dimensionless oscillation radius (R/R_0) and (b) the bubble collapse strength (k) and absorbed ultrasonic energy (E_u) under different ultrasonic pressure amplitudes (P_a) . The water temperature is 20°C. Here, $f_0=60$ kHz and $R_0=10~\mu m$.

As shown in Fig. 1b, during the expansion phase, the wall velocity initially increases slowly and then decreases until it reaches zero. Following this, in the collapse stage, the bubble wall velocity increases sharply in the reverse direction, undergoing violent oscillations and attenuation during the rebound attenuation stage.

The intra-bubble pressure P_{in} of a bubble consists primarily of air and water vapor pressures, while the extra-bubble pressure P_{out} encompasses the static pressure of the liquid, its viscous resistance, the bubble surface tension, and the ultrasonic pressure. As illustrated in Fig. 2, the changes in intra-bubble and extra-bubble pressures over one ultrasonic period are depicted.

The motion of the bubble walls is governed by the pressure difference between the intra-bubble and extra-bubble pressures. As illustrated in Fig. 2b, during the initial expansion stage, the intra-bubble pressure is slightly higher than the extra-bubble pressure, resulting in the outward expansion of the bubble walls. As the absolute value of the ultrasonic negative pressure decreases, the extra-bubble

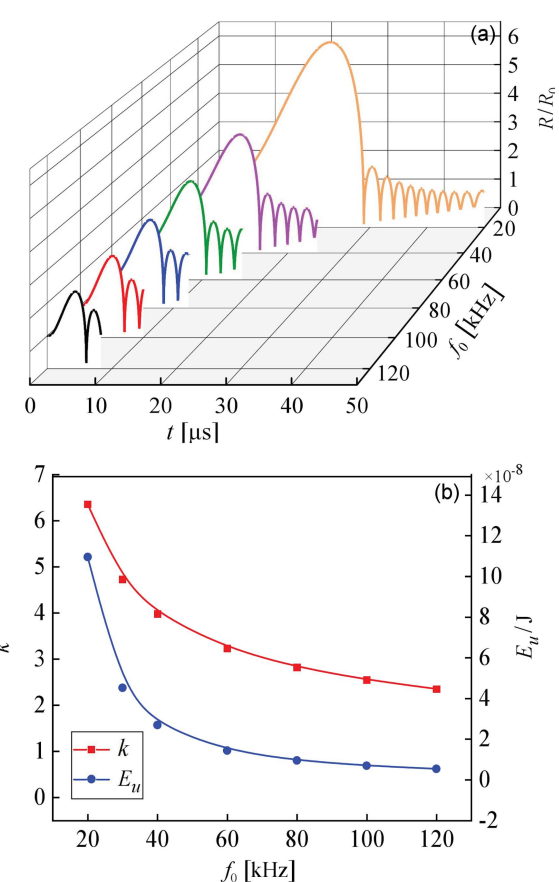


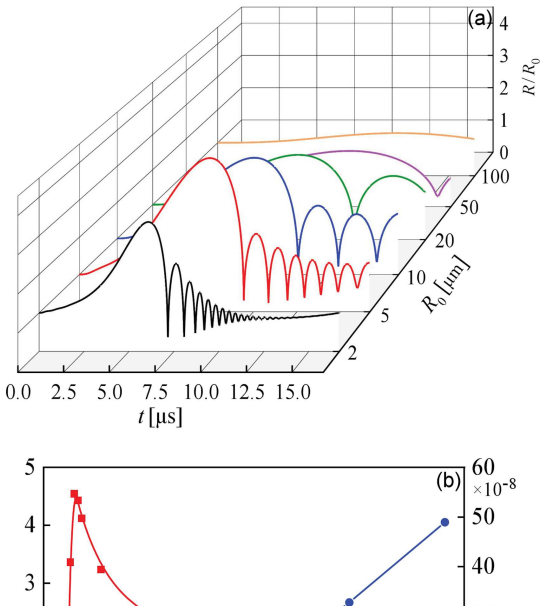
Fig. 4. (a) The time-dependent changes in the dimensionless oscillation radius (R/R_0) and (b) the bubble collapse strength (k) and absorbed ultrasonic energy (E_u) under different ultrasonic frequencies (f_0) . The water temperature is 20°C and $P_a=130$.

pressure increases until it exceeds the intra-bubble pressure. At this stage, the bubble walls begin to decelerate until they reach their maximum expansion. Following this, with a further increase of extra-bubble pressure, the bubble begins to collapse rapidly until it is compressed to its minimum size. During the collapse stage, the intra-bubble pressure can reach $\approx 2000~\mathrm{kPa}$. This preassure remains at a high value during the rebound attenuation stage due to the sudden change in bubble-wall velocity.

3.2. Analysis of influencing factors

3.2.1. Ultrasonic excitation parameters

The radial dynamics of ultrasonic bubbles is closely related to the ultrasonic excitation conditions and bubble sizes within a defined liquid medium. Figure 3 illustrates the variations of the dimensionless bubble oscillation radius over time during one ultrasonic period under different



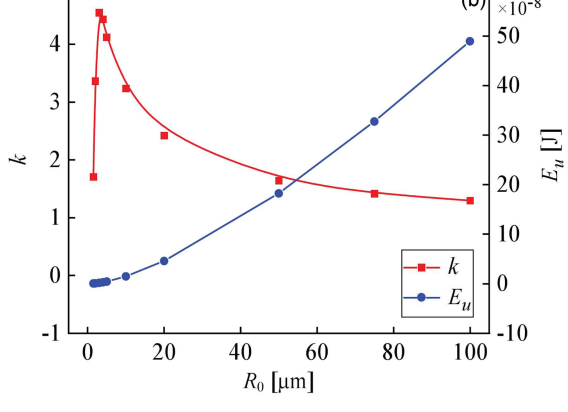


Fig. 5. (a) The time-dependent changes in the dimensionless oscillation radius (R/R_0) and (b) the bubble collapse strength (k) and absorbed ultrasonic energy (E_u) under different bubble initial radii (R_0) . The water temperature is 20°C. Here, $P_a=130$ kPa and $f_0=60$ kHz.

ultrasonic pressure amplitudes. Additionally, the bubble collapse strength and absorbed ultrasonic energy during the bubble expansion stage under various ultrasonic pressures are also presented. The ultrasonic frequency f_0 is 60 kHz, the initial bubble radius R_0 is 10 μ m, and the water temperature is 20°C. As shown in Fig. 3, when the ultrasonic pressure increases, the maximum oscillation radius, rebound radius, bubble collapse strength, and absorbed ultrasonic energy during the expansion phase — all increase. Additionally, the duration of both the expansion and collapse phases is prolonged, and the number of rebound attenuations decreases.

The radial dynamics characteristics of ultrasonically excited bubble at different ultrasonic frequencies are shown in Fig. 4. The ultrasonic pressure amplitude P_a is 130 kPa, and all other conditions remain the same as those in Fig. 3. It is evident that the effect of ultrasonic frequency f_0 on the radial motion characteristics of bubbles is significantly more pronounced compared to that of ultrasonic

pressure. Figure 4 shows that with the increase of f_0 , the maximum and rebound oscillation radius of the bubble decrease significantly, and the duration of expansion, collapse, and rebound attenuation stages is significantly shorter. The bubble collapse strength and absorbed ultrasonic energy are greatly reduced. The observed phenomena are attributed to the increasing inertia of the bubble during its oscillations. Additionally, as the ultrasonic frequency increases, its effect on the radial motion of the bubble steadily weakens. Although the radial dynamics characteristics of bubbles at lower frequencies (below 20 kHz) are not shown in Fig. 4, it can be expected that for a bubble with a determined initial radius, there is a specific frequency at which the bubble will oscillate most intensely.

Figure 5 illustrates the radial oscillation characteristics of bubbles with varying initial radii. The ultrasonic pressure amplitude P_a is 130 kPa, the frequency f_0 is 60 kHz, and the water temperature is 20°C. The varying intrinsic frequencies of bubbles with different initial radii result in significant differences in their radial oscillation characteristics. From Fig. 5, it is evident that bubbles with smaller initial radii absorb less ultrasonic energy, resulting in relatively weaker radial oscillation processes. On the other hand, larger bubbles absorb more energy; however, due to their greater inertia, it remains challenging to establish a distinctly dynamic process. Therefore, only bubbles within a specific initial radius range can experience significant radial dynamics, such as expansion, collapse, and rebound, when subjected to ultrasonic excitation. Additionally, changes in the bubble's initial radius and intrinsic frequency result in variations in its maximum and rebound oscillation radii. Consequently, the collapse strength of the bubble first increases and then decreases, while the absorbed ultrasonic energy continuously increases. The duration of the bubble expansion and collapse phases is extended — the first rebound point is shifted to the right, and the number of rebound attenuation oscillations decreases.

3.2.2. Liquid physical parameters

The liquid physical parameters, primarly viscosity, density, surface tension, and ultrasonic speed, also significantly affect the radial dynamics characteristics of bubbles and the effects of ultrasonic cavitation . Figure 6 illustrates the variations in collapse strength and absorbed ultrasonic energy of bubbles with an initial radius of 10 μ m under varying liquid physical parameters. The ultrasonic pressure amplitude P_a is 130 kPa, and the frequency f_0 is 60 kHz. As shown in Fig. 6, the bubble collapse strength and the absorbed ultrasonic energy decrease with increasing liquid viscosity, density,

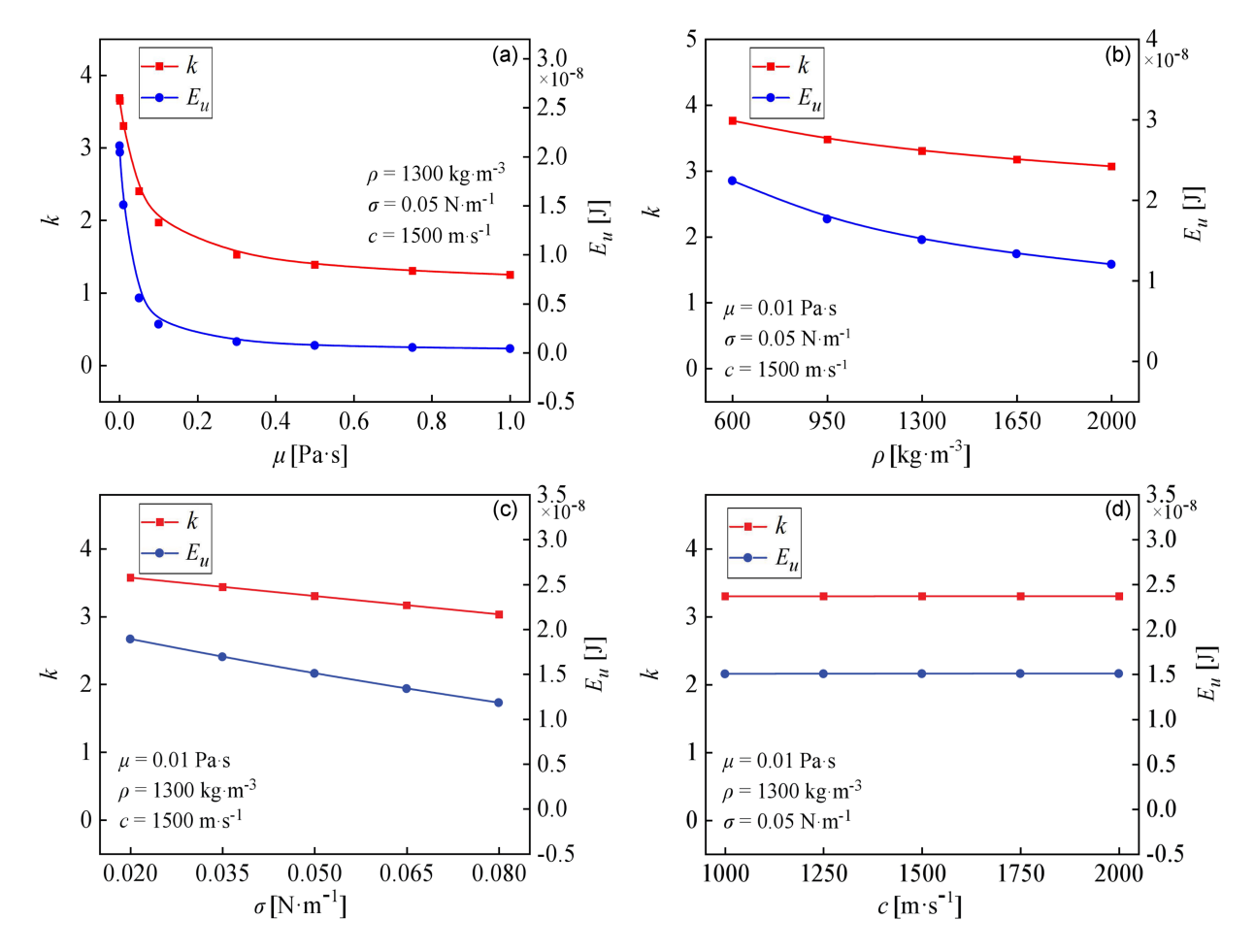


Fig. 6. The bubble collapse-strength (k) and absorbed ultrasonic energy (E_u) as functions of various liquid physical properties: (a) liquid viscosity, (b) liquid density, (c) surface tension and (d) ultrasonic speed in liquid. Here, $P_a=130$ kPa, $f_0=60$ kHz, and $R_0=10$ μ m.

and surface tension, while exhibiting minimal variation with ultrasonic speed. When the liquid viscosity is small, both the bubble collapse strength and absorbed ultrasonic energy change sharply with variations in liquid viscosity. However, the rate of these changes gradually becomes slower once the liquid viscosity exceeds a certain value, as shown in Fig. 6a.

3.3. Sensitivity analysis

The results of the above analysis demonstrate that radial dynamic behavior of bubbles is influenced by the physical parameters of the liquid, and the extent of this influence varies under different conditions. Next, we will conduct a sensitivity analysis to determine how sensitive the bubble collapse strength is to the physical parameters of the liquid.

The sensitivity coefficient is used to characterize the sensitivity of evaluation indicators to an influencing factor. A higher sensitivity coefficient

indicates a stronger relationship between the evaluation indicators and the influencing factor. The sensitivity coefficient is defined as

$$\gamma_i = \frac{(k_{i+1} - k_i)/k_i}{(L_{p,i+1} - L_{p,i})/L_{p,i+1}}, \quad i = 0, 1, ..., n,$$
 (6)

$$\gamma = \frac{1}{n} \sum_{i=0}^{n} \gamma_i,\tag{7}$$

where γ_i denotes the sensitivity coefficient of bubble collapse intensity to the liquid physical parameters for the *i*-th physical parameter, γ represents the average sensitivity coefficient of collapse intensity to physical parameters, k_i denotes the bubbles collapse intensity for the *i*-th physical parameter, and $L_{p,i}$ represents the value of the *i*-th physical parameter.

Figure 6 shows that the variations of bubble collapse strength with liquid viscosity exhibits strong nonlinear characteristics. Therefore, the sensitivity analysis of bubble collapse strength to the physical parameters of the liquid will be conducted in two different viscosity intervals, namely in a low-viscosity liquid ($\mu \in [0.0001, 0.1]$ Pa s) and a high-viscosity liquid ($\mu \in [0.1, 1]$ Pa s). The comparison

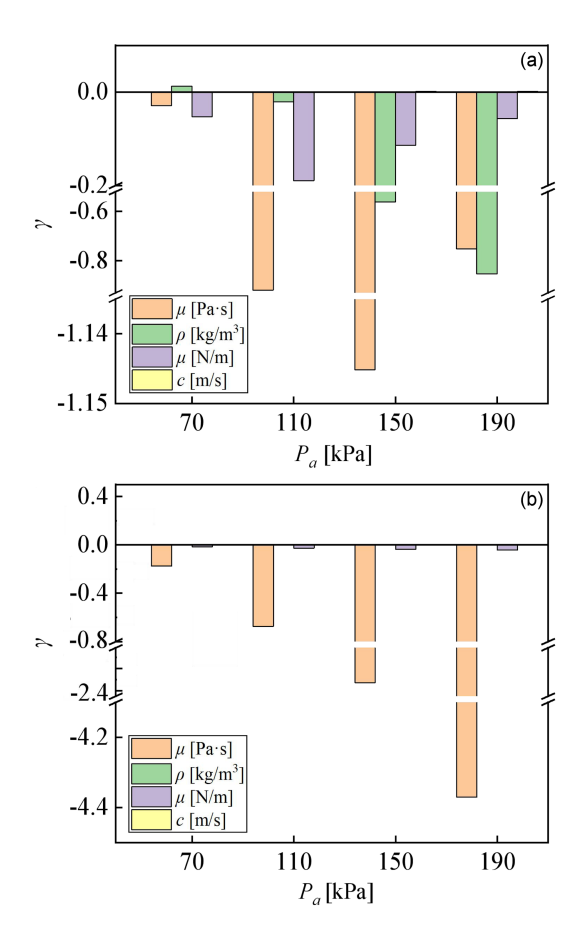


Fig. 7. Sensitivity coefficient of bubble collapse intensity to physical parameters under different pressure amplitudes (P_a) in different liquid: (a) low-viscosity liquid and (b) high-viscosity liquid. Here, $f_0=60$ kHz and $R_0=10~\mu\mathrm{m}$.

of the sensitivity coefficients of bubble collapse strength to the liquid physical parameters at different ultrasonic pressure amplitudes is presented in Fig. 7. The ultrasonic frequency f_0 is 20 kHz, and the bubble initial radius R_0 is 10 μ m.

Figure 7 illustrates that liquid viscosity μ is one of the most significant factors influencing the bubble collapse strength under various pressures amplitude P_a , particularly in high-viscosity liquids. In low-viscosity liquids, both the liquid density ρ and the surface tension σ also exhibit notable effects on the bubble collapse strength, whereas these effects are negligible in high-viscosity liquids. Moreover, the bubble collapse strength is relatively unaffected by the ultrasonic speed c across different P_a .

In low-viscosity liquids, bubble collapse strength is negatively correlated with μ and σ . Additionally, the sensitivity of bubble collapse strength to μ and σ varies with P_a , initially increasing and then decreasing as P_a rises. When P_a is low (70 kPa), collapse strength of bubbles is positively correlated with ρ , whereas it becomes negatively correlated at higher P_a . In high-viscosity liquids, the sensitivity of bubble collapse strength to μ increases

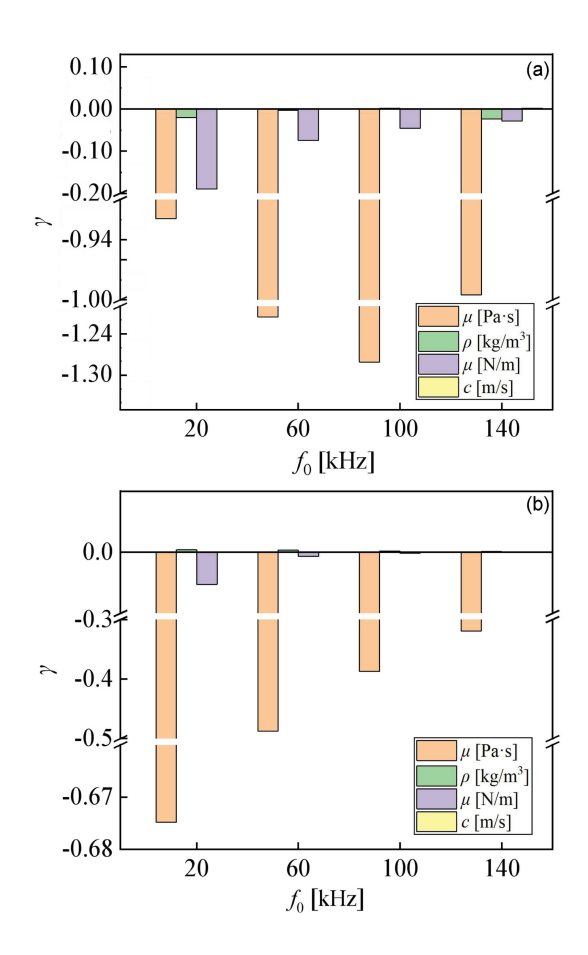


Fig. 8. Sensitivity coefficient of bubble collapse intensity to physical parameters under different ultrasonic frequencies (f_0) in different liquid: (a) low-viscosity liquid and (b) high-viscosity liquid. Here, $P_a=130$ kPa and $R_0=10~\mu{\rm m}$.

as P_a increases, whereas other physical parameters of the liquid have negligible effects. From Fig. 7, it can also be observed that in low-viscosity liquids, while μ is overall the most significant factor influencing bubble collapse strength, the physical parameters with the greatest impact on collapse strength differ under varying P_a . Specifically, at a preassure of 70 kPa, μ has the most significant effect, whereas at 190 kPa, ρ becomes the dominant factor. Additionally, the sensitivity ranking of bubble collapse strength to physical parameters of the liquid changes with varying P_a .

Figure 8 presents a comparison analysis of the sensitivity coefficients of bubble collapse strength with respect to physical parameters of the liquid under varying ultrasonic frequencies. The ultrasonic pressure amplitude is 130 kPa, and the initial bubble radius is 10 μ m.

As shown in Fig. 8, the liquid viscosity μ is the most critical factor influencing the bubble collapse strength across varying ultrasonic frequencies f_0 . The surface tension σ also plays a significant role in the collapse-strength process under different f_0 . However, the role of liquid density ρ is relatively

limited, while the ultrasonic speed c has a minimal impact. Overall, the sensitivity of the bubble collapse strength in low-viscosity liquids is greater than that in high-viscosity liquids.

In low-viscosity liquids, the sensitivity coefficients of bubble collapse strength to liquid viscosity μ exhibit an initial increase before decreasing as the ultrasonic frequency f_0 rises, whereas the sensitivity coefficients of collapse strength to surface tension σ continuously decrease. In high-viscosity liquids, the sensitivity of bubble collapse strength to both μ and σ diminishes with increasing f_0 , indicating that the influence of liquid physical parameters on bubble collapse strength gradually weakens as f_0 increases. Additionally, the liquid density ρ and the ultrasonic speed c have minimal influence on bubble collapse strength, and the relationships between these parameters and bubble collapse strength (whether positive or negative) depend strongly on f_0 .

Analysing the sensitivity of bubble dynamic characteristics in response to liquid physical parameters under ultrasound excitation is crucial for improving the performance of sonochemical reactors and ultrasound medical devices. In particular, buble vibration and collapse release energy that directly affect the rate of chemical reactions. By adjusting the physical properties of the liquid, it is possible to optimize reactor conditions, enhancing both the rate and yield of chemical reactions and reducing the associated costs. Additionally, encapsulated bubbles can serve as drug carriers, achieving targeted drug release under ultrasound excitation. Investigating the sensitivity of bubble dynamics to liquid property parameters can help optimize drug delivery systems and enable more efficient and precise drug release.

4. Conclusions

We examined the factors influencing the radial dynamic characteristics of bubbles, focusing on the ultrasonic energy absorbed by the bubble. Furthermore, we examined the sensitivity relationships between the radial dynamic characteristics of bubbles and the physical parameters in liquids of varying viscosity.

The radial dynamic characteristics of bubbles are influenced by a combination of ultrasonic excitation parameters, bubble size, and physical properties of the liquid. The maximum and rebound oscillation radius of a bubble, as well as its collapse strength and the absorbed ultrasonic energy, increase with increasing ultrasonic pressure but decrease with increasing ultrasonic frequency. The influence of ultrasonic frequency on these characteristics is significantly more pronounced than that of ultrasonic pressure. Under specific ultrasonic excitation conditions, only bubbles whose initial radius

falls within a certain range exhibit notable radial dynamic behavior. As the initial radius increases, the bubble's maximum and rebound oscillation radius, along with its collapse strength, initially rise and subsequently decline.

The sensitivity of bubble collapse strength to the physical parameters of the liquid under various ultrasonic excitation conditions is complex and multifaceted for both low- and high-viscosity liquids. Generally, liquid viscosity is the primary factor influencing bubble collapse strength. Additionally, liquid density and surface tension also exhibit noticeable effects on collapse strength under specific conditions. However, ultrasonic speed demonstrates minimal impact on collapse strength.

Acknowledgments

This study was supported by the BP Key Program (grant No. 2024X019-KXZ), the National Natural Science Foundation of China (grant No. 52276026), and the State Key Laboratory of Acoustics and Marine Information, Chinese Academy of Sciences (grant No. SKLA202411).

References

- [1] J. Rooze, E.V. Rebrov, J.C. Schouten, J.T.F. Keurentjes, *Ultrason. Sonochem.* **20**, 1 (2013).
- [2] R.J. Wood, J. Lee, M.J. Bussemaker, *Ultrason. Sonochem.* **38**, 351 (2017).
- [3] X. Ren, C. Li, F. Yang, Y. Huang, C. Huang, K. Zhang, L. Yan, J. Food Eng. 265, 109697 (2020).
- [4] Y. Dai, S. Li, M. Feng, B. Chen, J. Qiao, Materials 17, 5185 (2024).
- [5] J. Choi, J. Khim, B. Neppolian, *Ultrason. Sonochem.* 51, 412 (2019).
- [6] W. Lei, A. Li, K. Zhou, J. Hu, S. Qian, Phys. Fluids 36, 051912 (2024).
- [7] Z. Liu, M. Yang, W. Yao, T. Wang, G. Chen, *Chem. Eng. Sci.* 280, 119052 (2023).
- [8] M. Wang, Y. Zhou, *Ultrason. Sonochem.* 42, 327 (2018).
- [9] C. Kalmár, K. Klapcsik, F. Hegedűs, *Ultrason. Sonochem.* 64, 104989 (2020).
- [10] K. Kerboua, O. Hamdaoui, *Ultrason. Sonochem.* 41, 449 (2018).
- [11] W. Lauterborn, T. Kurz, Rep. Prog. Phys. 73, 106501 (2010).
- [12] B. Wang, T. Zeng, J. Shang, J. Tao, Y. Liu, T. Yang, H. Ren, G. Hu, J. Water Process Eng. 63, 105470 (2024).

- [13] W. Lauterborn, R. Mettin, in: *Power Ultrasonics*, 2nd ed., Eds. J.A. Gallego-Juárez, K.F. Graff, M. Lucas, Elsevier, 2023, Ch. 3, p. 23.
- [14] S. Behnia, A. Jafari, W. Soltanpoor, O. Jahanbakhsh, Chaos Solitons Fract. 41, 818 (2009).
- [15] H. A. Kafiabad, K. Sadeghy, J. Non-Newtonian Fluid Mech. 165, 800 (2010).
- [16] X. Zhong, J. Eshraghi, P. Vlachos, S. Dabiri, A.M. Ardekani, *Int. J. Multi-phase Flow* 132, 103433 (2020).
- [17] A. Dehane, S. Merouani, O. Hamdaoui, A. Alghyamah, *Ultrason. Sonochem.* 73, 105498 (2021).
- [18] K. Peng, F. G. F. Qin, R. Jiang, S. Kang, Ultrason. Sonochem. 69, 105253 (2020).
- [19] X. Wang, Z. Ning, M. Lv, C. Sun, Results Phys. 25, 104226 (2021).
- [20] A.A. Doinikov, *Phys. Fluids* **14**, 1420 (2002).
- [21] Y. Ma, H. Chen, Appl. Acoust. 146, 76 (2019).
- [22] Y. Zhang, S. Li, *Ultrason. Sonochem.* **35**, 431 (2017).
- [23] X. Wang, Z. Ning, M. Lv, C. Sun, Results Phys. 29, 104727 (2021).
- [24] G. Matafonova, V. Batoev, *Water Res.* **182**, 116016 (2020).
- [25] Y. Wang, D. Chen, P. Wu, J. Li, *Phys. Fluids* 36, 046109 (2024).

- [26] S. Merouani, O. Hamdaoui, Z. Boutamine, Y. Rezgui, M. Guemini, *Ultrason.* Sonochem. 28, 382 (2016).
- [27] R. Sadighi-Bonabi, N. Rezaee, H. Ebrahimi, M. Mirheydari, *Phys. Rev. E* 82, 016316 (2010).
- [28] X. Wang, Z. Ning, M. Lv, P. Wu, C. Sun, Y. Liu, *Ultrason. Sonochem.* 92, 106271 (2023).
- [29] Y. Ma, G. Zhang, T. Ma, *Ultrason.* Sonochem. **84**, 105953 (2022).
- [30] J. Liang, J. Liu, *Ultrason. Sonochem.* 96, 106428 (2023).
- [31] C. Guo, J. Wang, X. Li, S. Yang, W. Li, Chem. Eng. Process. Process Intensif. 199, 109765 (2024).
- [32] L. Rayleigh, Lond. Edinb. Dubl. Philos. Mag. J. Sci. 34, 94 (1917).
- [33] M. Plesset, J. Appl. Mech. 16, 277 (1949).
- [34] B.E. Noltingk, E.A. Neppiras, *Proc. Phys. Soc. B* **63**, 674 (1950).
- [35] J.B. Keller, M. Miksis, J. Acoust. Soc. Am. 68, 628 (1980).
- [36] F. Hegedűs, K. Klapcsik, W. Lauterborn, U. Parlitz, R. Mettin, *Ultrason. Sonochem*. 67, 105067 (2020).
- [37] L. Ye, X. Zhu, Y. Liu, *Ultrason. Sonochem.* **59**, 104744 (2019).